

The collective oscillation period of inter-coupled Goodwin oscillators

Yongqiang Wang, Yutaka Hori, Shinji Hara *Fellow, IEEE*, Francis J. Doyle III *Fellow, IEEE*

Abstract—Many biological oscillators are arranged in networks composed of many inter-coupled cellular oscillators. However, results are still lacking on the collective oscillation period of inter-coupled gene regulatory oscillators, which, as has been reported, may be different from the oscillation period of an autonomous cellular oscillator. Based on the Goodwin oscillator, we analyze the collective oscillation pattern of coupled cellular oscillator networks. First we give a condition under which the oscillator network exhibits oscillatory and synchronized behavior, then we estimate the collective oscillation period based on a multivariable harmonic balance technique. Analytical results are derived in terms of biochemical parameters, thus giving insight into the basic mechanism of biological oscillation and providing guidance in synthetic biology design. Simulation results are given to confirm the theoretical predictions.

I. INTRODUCTION

Diverse biological rhythms are generated by multiple cellular oscillators that somehow manage to operate synchronously. In systems ranging from circadian rhythms to segmentation clocks, it remains a challenge to understand how collective oscillation patterns (e.g., oscillation period, amplitude) arise from autonomous cellular oscillators. As has been reported in the literature, there can be significant differences between collective oscillation patterns and cell autonomous oscillation patterns, the difference are embodied not only in the oscillation amplitude [1], but also in the oscillation period [2], [3].

The famous Goodwin oscillator provides a perfect model to study the mechanism of how collective oscillation pattern arises from autonomous cellular oscillators. The Goodwin oscillator was proposed in 1965 to model the oscillatory behavior in enzymatic control processes [4], [5]. It is a minimal model that describes the oscillatory negative feedback regulation of a translated protein which inhibits its own transcription. Because the Goodwin oscillator can capture the essential characteristics in biochemical oscillators, it has been extensively used to model biological oscillators such as ultradian clocks of vertebrate embryos [6] and circadian clocks of neurospora [7], drosophila [8] as well as mammals [9].

The work was supported in part by Institute for Collaborative Biotechnologies under grant W911NF-09-D-0001, U.S. Army Research Office under grant W911NF-07-1-0279, National Institutes of Health under grant GM078993, and Grant-in-Aid for JSPS Fellows of Japan Society for the Promotion of Science (JSPS) under grant No. 23-9203. The content of the information does not necessarily reflect the position or the policy of the Government, and no official endorsement should be inferred.

Yongqiang Wang, Francis J. Doyle III are with Department of Chemical Engineering, University of California, Santa Barbara, California 93106-5080 USA. E-mail: wyqthu@gmail.com, frank.doyle@icb.ucsb.edu.

Yutaka Hori and Shinji Hara are with Department of Information Physics and Computing, The University of Tokyo, Tokyo 113-8656 Japan. E-mail: Yutaka_hori@ipc.i.u-tokyo.ac.jp, Shinji_hara@ipc.i.u-tokyo.ac.jp.

Another advantage of the Goodwin oscillator is that it allows for an analytical understanding of the basic dynamical mechanisms, whereas other biophysically substantiated models of cellular oscillators usually exhibit high complexity and large number of variables, which hamper the mathematical treatment, and subsequently obscure the underlying mechanisms. The Goodwin oscillator allows one to gain insights into the mechanisms of biochemical rhythms. For example, the oscillation conditions of a single Goodwin oscillator were obtained in [10], [11], [12], [13]. The synchronization conditions for coupled Goodwin oscillator networks were reported in [14], [15], [16]. Based on a multivariable harmonic balance technique, the oscillation patterns of a single Goodwin oscillator were obtained in [17], [18]. This is an important step toward understanding the period determination in biochemical oscillators. However, given that biological rhythms are generated by **multiple** cellular oscillators coupled through intercellular signaling, it remains a challenge to determine the periods in biological rhythms, which ranges from seconds in cardiac cell contraction to years in reproduction. Recently, using the phenomenological phase model, the authors in [19] proved that if the intercellular coupling is weak, the collective period is identical to the autonomous period. However, since the phase model contains no direct biological mechanism of the cellular clock, it can potentially weaken the model's reliability in checking scientific hypotheses.

This paper derives analytical results for the collective oscillation period of multi-cellular networks based on coupled Goodwin oscillators. Specifically, we study the collective period of a network of Goodwin oscillators connected by diffusive coupling. The basic idea is to use a multivariable harmonic balance technique [20]. In fact, due to the multi-cellular structure, the solution to harmonic balance equations in the multivariable harmonic balance technique is very difficult to obtain. Here we are interested in the collective period, so we can circumvent the problem by restricting our attention to solutions corresponding to synchronized oscillations in the oscillator network. To this end, we also give an oscillation/synchronization condition for the Goodwin oscillator network.

II. MODEL DESCRIPTION AND TRANSFORMATION

The Goodwin oscillator describes the dynamics of an oscillatory negative feedback regulation loop. As shown in Fig. 1, mRNA X_1 produces a protein X_2 which, in turn, activates a transcriptional inhibitor X_3 . The inhibitor X_3 inhibits the production of mRNA X_1 , which closes a negative feedback loop. The kinetic dynamics of the Goodwin oscillator are

given by [4], [10], [21]:

$$\begin{cases} \frac{d[X_1]}{dT} = \frac{v_0}{1 + ([X_3/K_m]^p)} - k_1[X_1] \\ \frac{d[X_2]}{dT} = v_1[X_1] - k_2[X_2] \\ \frac{d[X_3]}{dT} = v_2[X_2] - k_3[X_3] \end{cases} \quad (1)$$

Here $[X_1]$, $[X_2]$, and $[X_3]$ are concentrations of mRNA X_1 , protein X_2 , and inhibitor X_3 , respectively; v_0 , v_1 , and v_2 are the rates of transcription, translation, and catalysis; k_1 , k_2 , and k_3 are rate constants for degradation of each component; $1/K_m$ is the binding constant of end product to transcription factor; and p is Hill coefficient, which describes cooperativity of end product repression.

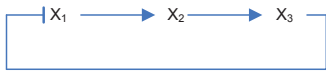


Fig. 1. **Schematic diagram of a Goodwin oscillator.** The mRNA X_1 produces a protein X_2 which, in turn, activates a transcriptional inhibitor X_3 . The inhibitor X_3 inhibits the production of X_1 , which closes a negative feedback loop.

There are other interpretations of the above Goodwin oscillator [4], for example, one may regard X_2 as an enzyme precursor that after primary synthesis on mRNA templates, X_1 , passes through a pool of inactive molecules before being transformed into mature, active enzyme, X_3 . One may also take X_1 to be an enzyme population whose rate of synthesis is regulated by feedback control at the polysome level via a metabolite X_3 . In this case, X_2 is then an intermediate in the biosynthetic sequence leading to X_3 .

The Goodwin oscillator (1) can be transformed into

$$\begin{cases} \frac{dx_1}{dt} = f(x_3) - b_1 x_1 \\ \frac{dx_2}{dt} = x_1 - b_2 x_2 \\ \frac{dx_3}{dt} = x_2 - b_3 x_3 \end{cases}, \quad f(x) = \frac{1}{1 + x^p} \quad (2)$$

via the introduction of dimensionless variables

$$\varsigma = \sqrt[3]{\frac{K_m}{v_0 v_1 v_2}}, \quad x_1 = \frac{\varsigma^2 v_1 v_2 [X_1]}{K_m},$$

$$x_2 = \frac{\varsigma v_2 [X_2]}{K_m}, \quad x_3 = \frac{[X_3]}{K_m}, \quad t = \frac{1}{\varsigma} T$$

In (2), b_1 , b_2 , and b_3 are positive parameters given by

$$b_i = k_i \varsigma, \quad i = 1, 2, 3$$

Suppose the oscillator network is composed of N oscillators, and they are connected by diffusive coupling, then the

dynamics of the network are given by

$$\begin{cases} \frac{dx_{1,i}}{dt} = f(x_{3,i}) - b_1 x_{1,i} \\ \frac{dx_{2,i}}{dt} = x_{1,i} - b_2 x_{2,i} - \sum_{j=1}^N a_{i,j} (x_{2,i} - x_{2,j}) \\ \frac{dx_{3,i}}{dt} = x_{2,i} - b_3 x_{3,i} \end{cases} \quad (3)$$

where $i = 1, 2, \dots, N$ denotes the index of the i th oscillator, and $a_{i,j} \geq 0$ denotes the coupling strength between oscillator i and oscillator j . If $a_{i,j} = 0$, then there is no interaction between oscillator i and oscillator j .

Assumption 1: We assume that the interaction is bidirectional, i.e., $a_{i,j} = a_{j,i}$. We also assume that the interaction topology is connected, i.e., there is a multi-hop path (i.e., a sequence with nonzero values $a_{i,m_1}, a_{m_1,m_2}, \dots, a_{m_{p-1},m_p}, a_{m_p,j}$) from each node i to every other node j .

Remark 1: Since protein is usually diffusible and involved in intercellular signaling [22], we model the intercellular coupling by the diffusion of x_2 , which usually represents the protein product in the Goodwin oscillator model.

For convenience in analysis, we can write (3) into the following matrix form:

$$\begin{cases} \frac{dX_1}{dt} = \vec{f}(X_3) - b_1 X_1 \\ \frac{dX_2}{dt} = X_1 - b_2 X_2 - A X_2 \\ \frac{dX_3}{dt} = X_2 - b_3 X_3 \end{cases} \quad (4)$$

where

$$X_i = \begin{bmatrix} x_{i,1} \\ x_{i,2} \\ \vdots \\ x_{i,N} \end{bmatrix}, \quad i = \{1, 2, 3\}, \quad \vec{f}(X_3) = \begin{bmatrix} f(x_{3,1}) \\ f(x_{3,2}) \\ \vdots \\ f(x_{3,N}) \end{bmatrix}, \quad (5)$$

$$A = \begin{bmatrix} \sum_{j \neq 1} a_{1,j} & -a_{1,2} & \dots & -a_{1,N} \\ -a_{2,1} & \sum_{j \neq 2} a_{2,j} & \dots & -a_{2,N} \\ \vdots & \ddots & \ddots & \vdots \\ -a_{N,1} & \dots & -a_{N,N-1} & \sum_{j \neq N} a_{N,j} \end{bmatrix} \quad (6)$$

Next, based on a multivariable harmonic balance technique, we will analyze the collective period of the Goodwin oscillator network in (4).

III. OSCILLATION/SYNCHRONIZATION CONDITION

To study the collective period, we need to guarantee that the component elements in X_i ($i = \{1, 2, 3\}$) in (4) first oscillate, and then further more, oscillate in synchrony. In this paper, we consider the Y-oscillation, which is defined as follows [20]:

Definition 1: A system $\dot{x} = f(x)$ with $x(t) \in \mathcal{R}^m$ is said to be Y-oscillatory if each solution is bounded and there

exists a state variable x_i such that $\lim_{t \rightarrow +\infty} x_i(t) < \overline{\lim}_{t \rightarrow +\infty} x_i(t)$ for almost all initial states $x(0)$.

To prove that (4) is Y-oscillatory, we introduce Lemma 1:

Lemma 1: [23] System (4) is Y-oscillatory if all conditions (a), (b), and (c) hold:

- (a) It only has isolated equilibria X^* ;
- (b) The positive semiorbit $\{X(t) \triangleq [X_1(t), X_2(t), X_3(t)] | t \geq 0 \text{ and } t \in \text{dom}X(\bullet)\}$ is bounded;
- (c) The Jacobian matrix evaluated at the equilibrium point X^* , i.e., J , has at least one eigenvalue with positive real part.

Proof: The Lemma can be obtained by combining Theorem 1 in [23] and the discussion below its proof which shows that the hyperbolicity condition can be relaxed. ■

In the following, we will prove that (4) satisfies all the conditions in Lemma 1, and hence is Y-oscillatory. We will also give a synchronization condition for the oscillation. In this manuscript, we define synchronization as follows:

Definition 2: System (4) is synchronized if the elements in X_3 satisfy $\lim_{t \rightarrow +\infty} |x_{3,i}(t) - x_{3,j}(t)| = 0$ for any $1 \leq i, j \leq N$.

Remark 2: Only $x_{3,i}$ ($i = 1, 2, \dots, N$) is used in the definition of synchronization. This is because according to the modeling assumption, $x_{3,i}$ is corresponding to the concentration of inhibitor or enzyme, which can be regarded as the output of an Goodwin oscillator. Note that under this definition, when the system is synchronized, $x_{1,i}$ ($i = 1, 2, \dots, N$) may be identical or non-identical. The same situation holds for $x_{2,i}$ ($i = 1, 2, \dots, N$).

Theorem 1: (4) has oscillatory solutions if it satisfies the following inequality

$$R \triangleq \frac{pb_1^2 b_2^2 b_3^2 x_0^{p+1}}{(b_1 + b_2 + b_3)(b_1 b_2 + b_2 b_3 + b_1 b_3) - b_1 b_2 b_3} > 1 \quad (7)$$

where x_0 is the unique positive solution to $1/(1 + x_0^p) = b_1 b_2 b_3 x_0$. Furthermore, the oscillations in all oscillators are synchronized if the algebraic connectivity ϱ (which is defined as the second smallest eigenvalue of matrix A in (6)) of coupling topology satisfies

$$\varrho > -b_1 + \frac{\gamma}{4b_2 b_3}, \quad \gamma = \max_{x \geq 0} \left\{ \frac{px^{p-1}}{(1+x^p)^2} \right\} \quad (8)$$

Proof: From Lemma 1, we know to guarantee a Y-oscillatory solution, we need to prove the conditions (a), (b), and (c), are satisfied. The proof is decomposed into three steps.

Step I – Satisfaction of condition (a): Using the monotonic property of $f(\bullet)$, we can prove that (3) has only one equilibrium point $X_3^* = [x_0 \ x_0 \ \dots \ x_0]^T$ with $x_0 > 0$ determined by $f(x_0) = b_1 b_2 b_3 x_0$. The derivation is as follows:

In the equilibrium point, we have

$$\frac{dX_i^*}{dt} = 0, \quad i = \{1, 2, 3\}$$

So after some simple algebra, (4) is reduced to

$$\vec{f}(X_3^*) - b_1 b_2 b_3 X_3^* = b_1 b_3 A X_3^* \quad (9)$$

where $\vec{f}(X_3^*)$ and A are defined in (5) and (6), respectively. To prove the uniqueness of the equilibrium point, we only need to prove that (9) has a unique solution.

To this end, we check equation (9) element-wisely. Making use of the structure of matrix A in (6), we have the following equation for all $i = 1, 2, \dots, N$:

$$g(x_{3,i}^*) \triangleq f(x_{3,i}^*) - b_1 b_2 b_3 x_{3,i}^* = b_1 b_3 \sum_{j \neq i} a_{i,j} (x_{3,i}^* - x_{3,j}^*) \quad (10)$$

Since the interaction is bi-directional, i.e., $a_{i,j} = a_{j,i}$, it follows

$$\sum_{i=1}^N g(x_{3,i}^*) = \sum_{i=1}^N \sum_{j \neq i} a_{i,j} (x_{3,i}^* - x_{3,j}^*) = 0 \quad (11)$$

Next, we prove that (12) holds by proving that both $\max_i \{g(x_{3,i}^*)\}$ and $\min_i \{g(x_{3,i}^*)\}$ are zero:

$$g(x_{3,1}^*) = g(x_{3,2}^*) = \dots = g(x_{3,N}^*) = 0 \quad (12)$$

Suppose to the contrary that (12) does not hold, and hence $\max_i \{g(x_{3,i}^*)\} > 0$ is satisfied since $\sum_{i=1}^N g(x_{3,i}^*) = 0$ holds according to (11). Represent the index that has the largest $g(x_{3,i}^*)$ among all i ($i = 1, 2, \dots, N$) as m . If there are multiple indices m satisfying $g(x_{3,m}^*) = \max_i \{g(x_{3,i}^*)\}$, then any one can be index m . Because $f(\bullet)$ is a decreasing function, it follows that $g(\bullet)$ is a decreasing function according to its definition on the left hand side of (10). So if the maximal $g(x_{3,i}^*)$ is attained when $i = m$, $x_{3,m}^*$ should be the smallest among $x_{3,1}^*, x_{3,2}^*, \dots, x_{3,N}^*$. Therefore, the right hand side of (10), i.e.,

$$b_1 b_3 \sum_{j \neq i} a_{m,j} (x_{3,m}^* - x_{3,j}^*) \quad (13)$$

should be non-positive, and hence $g(x_{3,m}^*)$ should be non-positive. This contradicts the fact that $g(x_{3,m}^*)$ is the largest among all $g(x_{3,i}^*)$ and it is positive (due to the constraint in (11)). Hence $\max_i \{g(x_{3,i}^*)\} = 0$ holds.

Similarly, we can prove that $\min_i \{g(x_{3,i}^*)\} = 0$ holds.

Therefore, we have (12), which further leads to

$$f(x_{3,i}^*) = b_1 b_2 b_3 x_{3,i}^*, \quad i = 1, 2, \dots, N \quad (14)$$

Given that $f(\bullet)$ is a monotonic decreasing function on \mathbb{R}_+ , it follows that the solution to (14) is unique and it satisfies

$$x_{3,1}^* = x_{3,2}^* = \dots = x_{3,N}^* = x_0 > 0, \quad f(x_0) = b_1 b_2 b_3 x_0 \quad (15)$$

Therefore the solution to (9) is unique, thus the equilibrium point is unique and hence isolated.

Step II – Satisfaction of condition (b): Following the derivations in [24], [25], we can easily get that condition (b) is satisfied.

Step III – Satisfaction of condition (c): The fact that J has at least one eigenvalue with positive real part is equivalent to the statement that the linearized system of (4) around the equilibrium point is strictly unstable. So instead of proving (c) directly, next we prove the strict instability of linearized system of (4) around the equilibrium point under condition (7). To this point, we transform (4) into the frequency domain as shown in Fig. 2, where $H(s)$ is given by

$$\begin{aligned} H(s) &= ((sI + b_1I)(sI + b_2I + A)(sI + b_3I))^{-1} \\ &= \frac{1}{(s + b_1)(s + b_3)}(sI + b_2I + A)^{-1} \end{aligned} \quad (16)$$

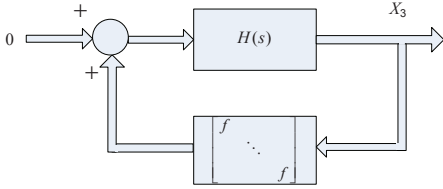


Fig. 2. Schematic diagram of the frequency domain formulation of (4).

Linearizing the nonlinear item $\vec{f}(X_3)$ in (4) around the equilibrium point $X_3^* = [x_0 \ x_0 \ \dots \ x_0]^T$ yields

$$\vec{f}(X_3) = \sigma X_3, \quad \sigma = -\frac{px_0^{p-1}}{(1+x_0^p)^2} = -px_0^{p-1}(b_1b_2b_3x_0)^2 \quad (17)$$

In the second equality, the relation $f(x_0) = b_1b_2b_3x_0$ at the equilibrium point is employed.

Based on the linearization in (17), we can get the closed-loop dynamics of the system in Fig. 2 as

$$G(s) = (I - \sigma H(s))^{-1}H(s) \quad (18)$$

Since A is a symmetric matrix, it only has real eigenvalues and it can always be diagonalized as follows:

$$A = P\Upsilon P^{-1}, \quad \Upsilon = \text{diag}(v_1, v_2, \dots, v_N) \quad (19)$$

where P is the similarity transformation matrix. Since A is the graph Laplacian, it always has an eigenvalue 0 associated with an eigenvector composed of identical elements [26]. Here we arrange the eigenvalues in increasing order, so $v_1 = 0$ always holds and the connectivity assumption in Assumption 1 leads to $v_i > 0$ ($i = 2, 3, \dots, N$) [26].

Substituting (19) into (16), we have

$$H(s) = P\Lambda P^{-1}, \quad \Lambda = \text{diag}(\lambda_1, \lambda_2, \dots, \lambda_N) \quad (20)$$

where eigenvalues λ_i ($i = 1, 2, \dots, N$) are given by

$$\begin{aligned} \lambda_1 &= \frac{1}{(s + b_1)(s + b_2)(s + b_3)} \\ \lambda_j &= \frac{1}{(s + b_1)(s + b_2 + v_j)(s + b_3)}, \quad j = 2, 3, \dots, N \end{aligned}$$

Using (18) and (20), we can obtain that

$$G(s) = P(I - \sigma\Lambda)^{-1}\Lambda P^{-1} = P\Delta P^{-1} \quad (21)$$

where

$$\Delta = \text{diag}(\delta_1, \delta_2, \dots, \delta_N)$$

with eigenvalues δ_i ($i = 1, 2, \dots, N$) given by

$$\delta_1 = \frac{\lambda_1}{1 - \sigma\lambda_1} = \frac{1}{(s + b_1)(s + b_2)(s + b_3) - \sigma} \quad (22)$$

$$\delta_j = \frac{\lambda_j}{1 - \sigma\lambda_j} = \frac{1}{(s + b_1)(s + b_2 + v_j)(s + b_3) - \sigma}, \quad (23)$$

where $j = 2, 3, \dots, N$.

According to the Routh–Hurwitz stability criterion, we know δ_1 is strictly unstable if and only if

$$\sigma < b_1b_2b_3 - (b_1 + b_2 + b_3)(b_1b_2 + b_1b_3 + b_2b_3) \quad (24)$$

is satisfied, and δ_j ($j = 2, 3, \dots, N$) is strictly unstable if and only if

$$\sigma < b_1(b_2 + v_j)b_3 - (b_1 + b_2 + v_j + b_3) \times (b_1(b_2 + v_j) + b_1b_3 + (b_2 + v_j)b_3) \quad (25)$$

is satisfied. Note that (24) is a necessary condition for (25), so $G(s)$ is strictly unstable if and only if (24) holds. Substituting σ in (17) into (24), we know that $G(s)$ is strictly unstable if and only if the inequality (7) in Theorem 1 holds, i.e., condition (c) holds if (7) is satisfied.

So far, we have proven conditions (a), (b), and (c), and hence guaranteed the existence of oscillatory solutions to (4). The synchronization condition for these oscillations, i.e., (8), follows easily from the secant condition in [14], thus the proof is omitted due to space limitations. Hence Theorem 1 is proven. ■

Remark 3: From (8), we can see that with an increase in γ , a stronger network connectivity ϱ is needed to guarantee network synchronization. Given that for $p > 1$, γ can be verified an increasing function of the Hill coefficient p , we know that a system having a higher Hill coefficient (i.e., higher end product cooperativity) requires a stronger coupling to maintain network synchronization.

IV. OSCILLATION PERIOD ESTIMATION BASED ON MULTIVARIABLE HARMONIC BALANCE TECHNIQUE

A. Oscillation analysis based on harmonic balance technique

In this section, we reformulate the problem of oscillation analysis using a multivariable harmonic balance technique [20]. This is motivated by the observation that $H(s)$ is a low pass filter thus higher order harmonics of oscillations in the close-loop system can be safely neglected. Hence the waveform of $x_{3,i}$ ($i = 1, 2, \dots, N$) can be approximated by its zero-order and first-order harmonic components [20], [27]:

$$x_{3,i} = \alpha_i + \beta_i \sin(\omega t + \phi_i), \quad i = 1, 2, \dots, N \quad (26)$$

where α_i and β_i denote the amplitudes of the zero-order and the first-order harmonic components, respectively, and ω and ϕ_i denote the oscillation frequency and phase, respectively.

Since $f(\bullet)$ is a static nonlinear function, it can be approximated by its describing functions [27]:

$$f(x_{3,i}) \approx \xi_i \alpha_i + \eta_i \beta_i \sin(\omega t + \phi_i) \quad (27)$$

where

$$\xi_i = \frac{1}{2\pi\alpha_i} \int_{-\pi}^{\pi} f(\alpha_i + \beta_i \sin(t)) dt \quad (28)$$

$$\eta_i = \frac{1}{2\pi\alpha_i} \int_{-\pi}^{\pi} f(\alpha_i + \beta_i \sin(t)) \sin(t) dt \quad (29)$$

The describing function ξ_i is the gain of $f(\bullet)$ when the input is a constant value α_i and the output is approximated by its zero-order harmonic. The describing function η_i is the gain of $f(\bullet)$ when the input is a sinusoid of amplitude β_i and the output is approximated by its first-order harmonic [27].

Consequently, the closed-loop equations that α_i and β_i are expected to satisfy are given by [20]

$$(I - H(0)\Xi)\vec{\alpha} = 0 \quad (30)$$

and

$$(I - H(j\omega)\Pi)\vec{\beta} = 0 \quad (31)$$

respectively, where

$$\vec{\alpha} = \begin{bmatrix} \alpha_1 \\ \alpha_2 \\ \vdots \\ \alpha_N \end{bmatrix}, \vec{\beta} = \begin{bmatrix} \beta_1 e^{j\phi_1} \\ \beta_2 e^{j\phi_2} \\ \vdots \\ \beta_N e^{j\phi_N} \end{bmatrix}, \Xi = \text{diag}\{\xi_1, \dots, \xi_N\}, \Pi = \text{diag}\{\eta_1, \dots, \eta_N\}$$

Therefore, the problem of oscillation analysis reduces to finding $\vec{\alpha}$, $\vec{\beta}$, and ω satisfying (30) and (31). Note that (30) and (31) are referred to as harmonic balance equations.

Let Ξ^* and Π^* be constant matrices satisfying (30) and (31) simultaneously. Define two linear systems $G_0(s)$ and $G_1(s)$ as

$$\begin{aligned} G_0(s) &\triangleq (I - H(s)\Xi^*)^{-1}H(s), \\ G_1(s) &\triangleq (I - H(s)\Pi^*)^{-1}H(s) \end{aligned} \quad (32)$$

The systems $G_0(s)$ and $G_1(s)$ are obtained by replacing the nonlinearity $f(\bullet)$ with the constant gain computed from the describing functions. Thus, the two linear systems contain some information about the oscillations of the original nonlinear system. According to Iwasaki [20], the predicted oscillation at frequency ω is expected stable if both $G_0(s)$ and $G_1(s)$ are marginally stable with poles of $s = 0$ and $s = \pm j\omega$ on the imaginary axis, respectively (the rest in the open left half plane). Therefore, the problem of oscillation analysis can be reduced to the following problem:

Problem 1: For the coupled Goodwin oscillators in (4), find Ξ^* and Π^* that

- satisfy (30) and (31), respectively;
- and at the same time guarantee that $G_0(s)$ and $G_1(s)$ in (32) are marginally stable.

The solution is given in the next section.

B. Oscillation period of coupled Goodwin oscillators

According to [20], (30) and (31) are very difficult to solve since in general Ξ and Π depend on $\vec{\alpha}$ and $\vec{\beta}$. Bearing in mind that we are interested in the collective period, we can restrict our attention to solutions that describe synchronized oscillations of the oscillator network. This provides a clue to solve the problem: according to Definition 2, synchrony means that $x_{3,i}$ are identical, i.e., 1) the phases ϕ_i ($i = 1, 2, \dots, N$) are identical; 2) the amplitudes α_i and β_i ($i = 1, 2, \dots, N$) are identical. Given that ξ_i and η_i are determined by α_i and β_i , we further have the equality of all ξ_i and all η_i . Making use of these properties, we have Theorem 2:

Theorem 2: For the Goodwin oscillator network in (4), if the oscillation/synchronization condition in Theorem 1 is satisfied, then its collective period $T_{\text{collective}}$ is given by

$$T_{\text{collective}} = \frac{2\pi}{\omega} = \frac{2\pi}{\sqrt{b_1 b_2 + b_1 b_3 + b_2 b_3}} \quad (33)$$

Proof: According to the above analysis, we have

$$\vec{\alpha} = \alpha \vec{1}, \vec{\beta} = \beta \vec{1}, \Xi = \xi I_N, \Pi = \eta I_N \quad (34)$$

where α , β , ξ , and η are constants and $\vec{1}$ is given by:

$$\vec{1} = [1 \ 1 \ \dots \ 1]^T$$

Hence (30) and (31) reduce to

$$\left(\frac{1}{\xi}I - H(0)\right)\alpha \vec{1} = 0 \quad (35)$$

and

$$\left(\frac{1}{\eta}I - H(j\omega)\right)\beta \vec{1} = 0 \quad (36)$$

respectively, which further means that $\frac{1}{\xi}$ is the eigenvalue of $H(0)$ corresponding to the eigenvector with identical elements, and $\frac{1}{\eta}$ is the eigenvalue of $H(j\omega)$ corresponding to the eigenvector with identical elements.

From (20), we know the eigenvalues of $H(0)$ are $\lambda_1 = \frac{1}{b_1 b_2 b_3}$ and $\lambda_j = \frac{1}{b_1(b_2 + v_j)b_3}$ for $j = 2, 3, \dots, N$. Further notice that only λ_1 corresponds to eigenvectors with identical elements. Thus we have

$$\frac{1}{\xi} = \lambda_1 = \frac{1}{b_1 b_2 b_3} \quad (37)$$

Similarly, we can get that the eigenvalues of $H(j\omega)$ are $\lambda_1 = \frac{1}{(j\omega + b_1)(j\omega + b_2)(j\omega + b_3)}$ and $\lambda_j = \frac{1}{(j\omega + b_1)(j\omega + b_2 + v_j)(j\omega + b_3)}$ for $j = 2, 3, \dots, N$. Further notice that only λ_1 corresponds to eigenvectors with identical elements. Thus we have

$$\frac{1}{\eta} = \lambda_1 = \frac{1}{(j\omega + b_1)(j\omega + b_2)(j\omega + b_3)} \quad (38)$$

According to (29), η is real, thus the item on the right hand side of (38) must be real, i.e., its imaginary part is zero. Given that

$$\begin{aligned} (j\omega + b_1)(j\omega + b_2)(j\omega + b_3) &= b_1 b_2 b_3 - \omega^2(b_1 + b_2 + b_3) \\ &\quad + j\omega((b_1 b_2 + b_1 b_3 + b_2 b_3) - \omega^2) \end{aligned} \quad (39)$$

we have the imaginary part $jw((b_1b_2 + b_1b_3 + b_2b_3) - w^2)$ equal to 0, which further leads to

$$w^2 = b_1b_2 + b_1b_3 + b_2b_3 \quad (40)$$

and

$$\eta = b_1b_2b_3 - (b_1b_2 + b_1b_3 + b_2b_3)(b_1 + b_2 + b_3) \quad (41)$$

Hence we know the collective period is determined by (33).

But to prove Theorem 2, it remains to prove that the oscillation at estimated frequency is stable, i.e., $G_0(s)$ and $G_1(s)$ in (32) are marginally stable [20]. So we proceed to prove that: (1) $G_0(s)$ has one pole of $s = 0$ and the rest in the open left half plane and, (2) $G_1(s)$ has a pair of imaginary poles $s = \pm jw$ and the rest in the open left half plane.

Substituting Ξ and Π in (34) into (32) yields

$$G_0(s) = (I - \xi H(s))^{-1} H(s) \quad (42)$$

and

$$G_1(s) = (I - \eta H(s))^{-1} H(s) \quad (43)$$

with ξ and η given in (37) and (41), respectively.

We first consider $G_0(s)$ in (42). From (21), (22), and (23), we know the eigenvalues of $G_0(s)$ are given by

$$\delta_1 = \frac{1}{(s + b_1)(s + b_2)(s + b_3) - \xi},$$

$$\delta_j = \frac{1}{(s + b_1)(s + b_2 + v_j)(s + b_3) - \xi}, \quad j = 2, 3, \dots, N$$

Substituting ξ in (37) into the above equations, we know the poles of (42) are determined by the roots of

$$(s + b_1)(s + b_2)(s + b_3) - b_1b_2b_3 = 0 \quad (44)$$

and

$$(s + b_1)(s + b_2 + v_j)(s + b_3) - b_1b_2b_3 = 0 \quad (45)$$

for $j = 2, 3, \dots, N$.

It is clear that (44) has one root $s = 0$. And using the Routh–Hurwitz stability criterion, we can get that the other roots of (44) and all roots of (45) are in the open left half plane. Hence $G_0(s)$ is marginally stable.

Similarly, we can prove that the eigenvalues of $G_1(s)$ are

$$\delta_1 = \frac{1}{(s + b_1)(s + b_2)(s + b_3) - \eta}$$

and

$$\delta_j = \frac{1}{(s + b_1)(s + b_2 + v_j)(s + b_3) - \eta}$$

for $j = 2, 3, \dots, N$, with η given in (41). And hence its poles are determined by the roots of

$$(s + b_1)(s + b_2)(s + b_3) - b_1b_2b_3 + (b_1b_2 + b_1b_3 + b_2b_3)(b_1 + b_2 + b_3) = 0 \quad (46)$$

and

$$(s + b_1)(s + b_2 + v_j)(s + b_3) - b_1b_2b_3 + (b_1b_2 + b_1b_3 + b_2b_3)(b_1 + b_2 + b_3) = 0 \quad (47)$$

for $j = 2, 3, \dots, N$.

It can be verified that $s = \pm jw$ are two roots of (46). And using the Routh–Hurwitz stability criterion, it follows that the other roots of (46) and all roots of (47) are in the open left half plane. So $G_1(s)$ is marginally stable. Hence the derived oscillation at frequency w in (33) is stable, which completes the proof. ■

Remark 4: The collective period in (33) is given in terms of the dimensionless parameters in (2). Representing the collective period with the original dimensional parameters gives

$$T_{\text{collective}} = \frac{2\pi}{\sqrt{k_1k_2 + k_1k_3 + k_2k_3}} \quad (48)$$

Eqn. (48) means that the collective period decreases with an increase in the rate constants for degradation of each component, but it is independent of the rates of transcription, translation, and catalysis. These give insights into the basic determination mechanism of the collective period in coupled biological oscillator networks, and may further provide guidance in synthetic biology design.

Remark 5: From (48), we can see that when the intercellular interaction is of the form in (3), the collective period is only determined by k_1 , k_2 , and k_3 , and it is independent of intercellular coupling. The results are obtained based on analytical treatment of a network of coupled gene regulatory oscillators and they corroborate the results in [19], which are obtained using the phenomenological single-variable phase model and state that the strength of intercellular coupling does not affect the collective period of circadian rhythm oscillator networks.

Remark 6: It is worth noting that if the coupling is of a form different from (3), then it may affect the collective period, even if it is still of diffusive type. Examples have been reported in [2] and [3].

V. NUMERICAL STUDY

In this section, simulation results are given to confirm the theoretical predictions. We considered a network of nine Goodwin oscillators. The coupling strengths $a_{i,j}$ were randomly chosen from a uniform distribution on $[0, 1]$ and are given in Table I. It can be verified that the coupling topology is connected and the algebraic connectivity is $\rho = 2.4583$ (ρ is equal to the second smallest eigenvalue of interaction matrix A in (6), as defined in Theorem 1).

TABLE I
COUPLING TOPOLOGY $a_{i,j}$ ($1 \leq i, j \leq 9$, $i \neq j$) OF THE GOODWIN OSCILLATOR NETWORK

	1	2	3	4	5	6	7	8	9
1		0.3	0.5	0	0.6	0.2	0	0.7	0.8
2	0.3		0.7	0.2	0.1	0.8	0.3	0.1	0.5
3	0.5	0.7		0.3	0.6	0.2	0.6	0	0.8
4	0	0.2	0.3		0.4	0.6	0.2	0.9	0.1
5	0.6	0.1	0.6	0.4		0.2	0.7	0.3	0.8
6	0.2	0.8	0.2	0.6	0.2		0.1	0.9	0.3
7	0	0.3	0.6	0.2	0.7	0.1		0.4	0.5
8	0.7	0.1	0	0.9	0.3	0.9	0.4		0.8
9	0.8	0.5	0.8	0.1	0.8	0.3	0.5	0.8	

First we tested our oscillation/synchronization condition in Theorem 1. The results are summarized in Table II. It can be seen that oscillation/synchronization can be obtained only when the parameters satisfy $R > 1$ in (7).

TABLE II
TEST OF THE OSCILLATION/SYNCHRONIZATION CONDITION

p	b_1	b_2	b_3	R	Simulation results
17	0.4	0.4	0.4	1.7102	Oscillation/synchronization
17	0.5	0.5	0.5	1.6541	Oscillation/synchronization
17	0.6	0.6	0.6	1.5286	Oscillation/synchronization
17	0.7	0.7	0.7	1.3266	Oscillation/synchronization
17	0.8	0.8	0.8	1.0421	Oscillation/synchronization
17	0.85	0.85	0.85	0.8686	No oscillation/synchronization
17	0.9	0.9	0.9	0.676	No oscillation/synchronization
17	1.0	1.0	1.0	0.2620	No oscillation/synchronization
17	0.7	0.8	0.9	1.0433	Oscillation/synchronization
17	0.9	0.8	0.8	0.9300	No oscillation/synchronization

We also compared the collective periods in the oscillatory cases in Table II with the estimated value. The results are summarized in Table III. It can be seen that the estimated values approximate the actual collective periods very closely.

TABLE III
COMPARISON BETWEEN THE ESTIMATED COLLECTIVE PERIOD [S] AND THE ACTUAL COLLECTIVE PERIOD [S]

$b_1 = b_2 = b_3$	0.4	0.5	0.6	0.7	0.8
Actual value	10.68	8.00	6.31	5.23	4.53
Estimated value	11.35	7.26	6.05	5.19	4.54
Estimation error	6.27%	-9.25%	-4.12%	-0.76%	0.22%

VI. CONCLUSIONS

Underlying biological rhythms are networks of interacting cellular oscillators. How the collective oscillation patterns arise from autonomous cellular oscillations is poorly understood. The Goodwin oscillator is a quintessential model of biochemical oscillators based on negative feedback mechanisms. Based on a network of coupled Goodwin oscillators, we studied analytically the oscillation/synchronization condition and collective period of coupled biochemical oscillators by using a multivariable harmonic balance technique. We give an oscillation/synchronization condition of coupled Goodwin oscillators. The condition shows that a system having a higher Hill coefficient (corresponding to a higher cooperativity of end product repression) requires a stronger intercellular coupling to maintain network synchronization. We also analytically estimate the collective oscillation period of the oscillator network. The collective oscillation period is only dependent on the degradation rates of each component, and it is independent of the rate of transcription, translation, and catalysis. The results are confirmed by numerical simulations and may provide guidance in synthetic-biological-oscillator design. Given that the Goodwin oscillator has been successfully implemented *in vivo*, synthetic biology based testing of the predictions is promising. Experimental verification is also feasible in biological oscillators whose degradation/synthesis rates are tunable.

REFERENCES

- [1] O. V. Popovych and P. A. Tass. Macroscopic entrainment of periodically forced oscillatory ensembles. *Prog. Biophys. Mol. Biol.*, 105:98–108, 2011.
- [2] H. J. Wülsche, S. Bauer, J. Kreissl, O. Ushakov, N. Korneyev, F. Henneberger, E. Wille, H. Erzgrässer, M. Peil, W. Elsässer, and I. Fischer. Synchronization of delay-coupled oscillators: a study of semiconductor lasers. *Phys. Rev. Lett.*, 94:163901, 2005.
- [3] L. Herrgen, S. Ares, L. G. Morelli, C. Schröter, F. Jülicher, and A. C. Oates. Intercellular coupling regulates the period of the segmentation clock. *Curr. Biol.*, 20:1244–1253, 2010.
- [4] B. C. Goodwin. Oscillatory behavior in enzymatic control processes. *Adv. Enzyme Regul.*, 3:425–438, 1965.
- [5] B. C. Goodwin. An entrainment model for timed enzyme syntheses in bacteria. *Nature*, 209:479–481, 1966.
- [6] S. Zeiser, J. Müller, and V. Liescher. Modeling the Hes1 oscillator. *J. Comput. Biol.*, 14:984–1000, 2007.
- [7] P. Ruoff, M. Vinsjevik, C. Monnerjahn, and L. Rensing. The goodwin model: simulating the effect of light pulses on the circadian sporulation rhythm of *neurospora crassa*. *J. Theor. Biol.*, 209:29–42, 2001.
- [8] P. Ruoff, M. Vinsjevik, C. Monnerjahn, and L. Rensing. The goodwin oscillator: on the importance of degradation reactions in the circadian clock. *J. Biol. Rhythms*, 14:468–479, 1999.
- [9] D. Gonze, S. Bernard, C. Waltermann, A. Kramer, and H. Herzel. Spontaneous synchronization of coupled circadian oscillators. *Biophys. J.*, 89:120–129, 2005.
- [10] J. S. Griffith. Mathematics of cellular control processes: I negative feedback to one gene. *J. Theoret. Biol.*, 20:202–208, 1968.
- [11] A. Hunding. Limit-cycles in enzyme-systems with nonlinear negative feedback. *Biophys Struct Mech.*, 1:47–54, 1974.
- [12] J. Tyson. On the existence of oscillatory solutions in negative feedback cellular control processes. *J. Math. Biol.*, 13:311–315, 1975.
- [13] Y. Hori, T. Kim, and S. Hara. Existence criteria of periodic oscillations in cyclic gene regulatory networks. *Automatica*, 47:1203–1209, 2011.
- [14] G. Stan, A. Hamadeh, R. Sepulchre, and J. Goncalves. Output synchronization in networks of cyclic biochemical oscillators. In *Proc. American Contr. Conf.*, pages 3973 – 3978, USA, 2007.
- [15] J. S. Kim and F. Allgöwer. Nonlinear synchronization of coupled oscillators: the polynomial case. pages 339–351. Springer, 2007.
- [16] A. Hamadeh, G. Stan, R. Sepulchre, and J. Goncalves. Global state synchronization in networks of cyclic feedback systems. *IEEE Trans. Autom. Control*, 57:478–483, 2012.
- [17] P. Papp. Analysis of biochemical phase shift oscillators by a harmonic balancing technique. *J. Math. Biol.*, 25:203–224, 1976.
- [18] Y. Hori and S. Hara. Oscillation pattern analysis for gene regulatory networks with negative cyclic feedback. In *Proc. 49th IEEE Conf. Decision Control*, pages 5798–5803, Atlanta, USA, 2010.
- [19] C. Liu, D. Weaver, S. H. Strogatz, and S. M. Reppert. Cellular construction of a circadian clock: period determination in the Suprachiasmatic Nuclei. *Cell*, 91:855–860, 1997.
- [20] T. Iwasaki. Multivariable harmonic balance for central pattern generators. *Automatica*, 44:3061–3069, 2008.
- [21] C. Fall, E. Marland, J. Wagner, and J. J. Tyson, editors. *Computational Cell Biology*. Springer, New York, 2005.
- [22] D. A. Lauffenburger and J. J. Linderman, editors. *Receptors, models for binding, trafficking, and signaling*. Oxford University Press, New York, 1993.
- [23] A. Pogromsky, T. Glad, and H. Nijmeijer. On diffusion driven oscillations in coupled dynamical systems. *Int. J. Bifurcation Chaos*, 9:629–644, 1999.
- [24] J. Mallet-Paret and H. Smith. The poincaré-bendixson theorem for monotone cyclic feedback systems. *J. Dyn. Differ. Equ.*, 2:367–421, 1996.
- [25] H. El Samad, D. Del Vecchio, and M. Khammash. Repressilators and promotilators: loop dynamics in synthetic gene networks. In *Proc. 2005 American Contr. Conf.*, pages 4405–4410, Portland, USA, 2005.
- [26] R. Horn and C. Johnson. *Matrix analysis*. Cambridge University Press, London, 1985.
- [27] H. K. Khalil. *Nonlinear systems*. Prentice Hall, New Jersey, 2002.